Journal of Renewable Materials

Tech Science Press

DOI: 10.32604/jrm.2021.014364

ARTICLE

# Study on the Bonding Performance of the Moso Bamboo Dowel Welded to a Poplar Substrate Joint by High-Speed Rotation

**Suxia Li[1,2], Haiyang Zhang[1,*], Biqing Shu[1,3], Liangsong Cheng[1], Zehui Ju[1] and Xiaoning Lu[1,*]**

[1]College of Materials Science and Engineering, Nanjing Forestry University, Nanjing, 210037, China

[2]College of Furniture and Art Design, Central South University of Forestry and Technology, Changsha, 410004, China

[3]College of Civil Engineering, Yangzhou Polytechnic Institute, Yangzhou, 225127, China

[*]Corresponding Authors: Haiyang Zhang. zhynfu@njfu.edu.cn; Xiaoning Lu. Email: luxiaoning-nfu@126.com

Received: 21 September 2020 Accepted: 11 November 2020

## ABSTRACT

The wood friction welding technique with its high bonding strength, low cost, high efficiency, and without any adhesive has been increasing concern in China. Moso bamboo (*Phyllostachys pubescens*) and poplar (*Populus sp.*) are widely planted and used in the furniture industry, interior decoration, and wood structure construction in China. The aim of this work was to investigate the bonding performance of moso bamboo dowel rotation welded joints with different dowel/receiving hole diameter ratios. The results indicated that the ratio of dowel/receiving hole diameter was an important parameter that influenced the welding performance. The bonding strength of the bamboo-to-poplar welded joints at the optimal ratio of 10/7 was as high as 7.50 MPa, which was higher than that of the beech (*Fagus sylvatica, L.*), schima (*Schima superba*) dowels and PVAc glued joints. The temperature measurement results showed a peak temperature of bamboo dowel welding as high as 350–360°C. Some differences in the temperature curves between each dowel/hole diameter ratio group were observed at the three different hole depths, such as the friction time, peak temperatures, and stabilization time at the maximum temperature, which could explain the differences in welding strengths between different ratios. The SEM results showed the temperature-induced softening, melting and flowing of cell-interconnected polymer material in the wood and bamboo structure. In addition, the bamboo fibers (mainly vascular bundles) were wrapped to form a dense continuous bonding layer, similar to the reinforced concrete, thus producing a good bonding effect. The Fourier transform-infrared spectroscopy (FT-IR) analyses showed that the high temperature resulted in the increase of the lignin relative content due to the degradation reaction of cellulose in the welding zone, which improved the bonding properties.

## KEYWORDS

Moso bamboo; rotation welding; tensile strength; optimal ratio; poplar

## 1 Introduction

High-speed rotation-induced wood dowel welding, without the use of any adhesive, has been shown to yield wood joints of considerable strength [1–6]. This joining technology has been utilized for the bonding of wood for more than a decade. Similar to the observation in vibration welding [7], the mechanism of the mechanically-induced high-speed rotation wood welding involves temperature-induced softening and the flow of some components in the wood structure, mainly lignin and some hemicelluloses, consequently

leading to the high densification of the bonded interface [1,8–10]. This joining system has strong advantages for commercial purposes because of its simple operation, high strength, and low cost. Previous studies on high-speed wood dowel rotation welding reported that the bonding strength of welded dowels was comparable to or higher than that of polyvinyl acetate (PVAc) glued joints [1–3]. As a result, this technique can be applied in the assembly of objects, such as furniture, wood-based panels, wooden multi-layer beams, wooden floors, and house walls [11–15].

Pizzi et al. carried out many studies on different parameters influencing wood-dowel welding by high-speed rotation [1–6]. The results indicated that the wood species of dowel and substrate, dowel/substrate hole diameter ratio, and friction time were important parameters that significantly affected the bonding performance of wood dowel rotation welding, while the grain orientation of the substrate, rotation rate of the dowel, and the use of rough or smooth dowels did not have any significant influence [1–6]. Moreover, the 10 mm/8 mm (dowel/hole) diameter ratio (difference) was very nearly optimal, though a dowel/hole diameter ratio higher than 10/8 (1.25) did not yield better results [1–6].

China's fast-growing poplar (*Populus sp*.) afforestation area and moso bamboo (*Phyllostachys pubescens*) yield are the first in the world [16]. Fast-growing poplar is the first choice for short-term industrial timber in China, and it is also one of the three important fast-growing tree species in the world [17]. The application of poplar has increased in the field of wood structure construction engineering in China. The Chinese bamboo forest planting area accounts for 1/3 of the global bamboo forest area. China is the most important moso bamboo producer and has the most significant application area in the world [18,19]. Similar to wood, bamboo is also a kind of a renewable biomass composite material and the best substitute for wood because of its fast growing rate, large abundance, short cutting period, and fibrous characteristics [18]. Bamboo is a lignocellulosic material that consists of longitudinal vascular bundles and ground tissue, and does not have transverse cells like wood. Due to its special physical structure, bamboo not only has good longitudinal mechanical properties but also has a high strength-to-weight ratio [20–22]. Bamboo, like poplar and all the other woods, is mainly composed of hemicelluloses, cellulose, and lignin. Therefore, in recent years, more and more scholars have shown great interest in studying bamboo friction welding in China.

Hu et al. [23] reported the possibility of applying mechanically-induced vibration welding to the joining procedure of a wood-bamboo-wood laminated composite lumber. The results showed that the average tensile strength values of the composites can meet furniture industry and wood construction requirements. Zhang et al. [24,25] employed the linear friction welding technology to moso bamboo and optimized the welding parameters of linear mechanically welded outer-to-inner flattened moso bamboo through a large number of experiments. The results indicated that the vibration amplitude and the welding pressure both had a significant influence on the performance of the joint, while a welding time of 4–6 s did not yield higher strength test results comparable to that of wood linear friction welding. Zhang et al. [26] reported that the structure of the vascular bundles had a great influence on the final performance of the welded bamboo joints. The vascular bundles as a natural reinforcement could not be melted and broken in the welding process, and the material flow in the welding process was attributed to the other bamboo cells, which had an abundance of lignin.

Fast-growing poplar and poplar-based products are widely used in China for the construction of wood structures. The welding performance of moso bamboo dowel that is welded to fast-growing wood substrate by high-speed rotation has not been reported. The purpose of this study is to explore whether moso bamboo dowels with abundant vascular bundles and lignin content could be used as an alternative to wood dowels. Thus, this study determined the bonding performance and mechanism of the bamboo dowel to poplar substrate welded joints, which can provide a rapid, convenient, and environmentally-friendly assembly technology for wood construction. In addition, the optimal bamboo dowel/receiving hole diameter ratio

was also investigated. In order to explain the differences in welding strengths between the different dowel/hole diameter ratios and explore the bonding mechanism, the temperature progression at the welding interface during bamboo dowel rotation welding was surveyed, the interesting wounded surface of the welded bamboo dowel was observed by scanning electron microscopy (SEM), and the thermal alteration of bamboo were investigated by Fourier transform-infrared spectroscopy (FT-IR) analyses.

## 2 Experimental

### *2.1 Preparation of Materials*

Moso bamboo was obtained from the forest area of Nanjing Forestry University. The structure of raw moso bamboo is round and hollow, different from that of wood, as shown in Fig. 1. A five-year-old bamboo sample with a wall thickness of approximately 12 mm was chosen to make dowels as this is an age at which the moso bamboo is considered to be mature and is normally harvested for industrial usage [27]. The outer green and the inner yellow skin of the bamboo were removed (Fig. 1), and only the middle part was retained, which is the best material for bamboo dowels (nails) [18]. Beech (*Fagus sylvatica, L.*) dowels and schima (*Schima superba*) dowels served as the controls with smooth surfaces, both of which were purchased from the market. Similar to the beech dowel, the schima dowel is one of the most widely used wood dowels in furniture and wood structure assembly in China. All of the bamboo and wood dowels were 10 mm in diameter and 100 mm in length with a smooth surface, and were dried to 3–5% MC prior to welding. Poplar (*Populus* × *euramericana 'San Martino 'I-72*) were purchased from Huai'an City of Jiangsu Province. Fifteen-year-old fast-growing poplar was cut into sizes of 50 mm × 50 mm × 20 mm (length × width × height) to serve as substrate blocks. The blocks were dried to 10%–12% MC. The basic density and main chemical composition content of the moso bamboo, beech, schima, and poplar are shown in Tab. 1.

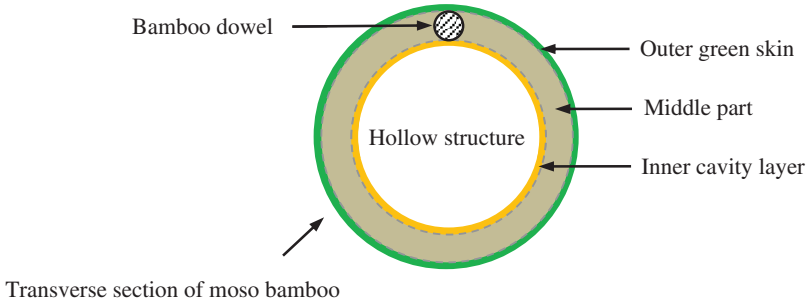


**Figure 1:** The processing part of a bamboo dowel from a moso bamboo

**Table 1:** Basic density and main chemical properties of bamboo, beech, schima and poplar

| Materials | Basic density (g/cm$^3$) | Lignin (%) | Cellulose (%) | Hemicellulose (%) |
|---|---|---|---|---|
| Moso bamboo [16] | 0.68 | 30.40 | 40.05 | 19.93 |
| Beech [28] | 0.72 | 29.05 | 43.80 | 24.82 |
| Schima [29] | 0.58 | 24.20 | 48.06 | 20.99 |
| Poplar [16] | 0.45 | 26.58 | 45.22 | 20.17 |

### 2.2 Production of Welded Joints by High-Speed Rotation-Induced Dowel Bonding

In order to find the best diameter ratio of bamboo dowel/receiving hole, approximately 40 bamboo dowels were welded to pre-drilled holes with a diameter of 9, 8, 7, or 6 mm in the poplar blocks by high-speed rotation. Additionally, in order to compare the welding strength of the bamboo-dowel and wood-dowel, 10 beech dowels and 10 schima dowels were inserted into through cylindrical pre-drilled holes with a diameter of 8 mm in the poplar blocks, because, according to the result of wood dowel rotation welding study, the optimal dowel/hole diameter ratio was near 10 mm/8 mm [1–6].

In addition, 10 other bamboo dowels were used to bond the poplar wood bases with the white latex (PVAc; Mastercraft, Carpoly, China) and served as controls. All of the bamboo dowels or wood dowels were inserted perpendicular to the transverse grain direction of the poplar substrate blocks using a high-speed fixed-base and a manually-operated drill (Type ZXJ–7016, Hangzhou West Lake, China). The dowels had a rotational rate of 1,500 rpm and a feed rate of 400–450 mm per min by manual insertion. Once the welded dowels came out through the bottom of the substrate blocks and exceeded about 5 mm in about 2–3 s, the rotation of the dowels was immediately stopped, and the pressure was maintained for approximately 3–5 s to allow fusion and bonding. PVAc had a pH value of 6.7, a solid content of 43.2%, and a viscosity of 0.63 Pa·s. According to the producer's recommendations, the double gluing technique was used in which the surfaces of both the receiving holes (10 mm in diameter) and bamboo dowels (10 mm in diameter) were coated with glue prior to the insertion of the dowels. All the welded specimens as well as the PVAc glued samples were conditioned for one week in an environmental chamber at a temperature of 20°C and relative humidity of 65% before tensile testing.

### 2.3 Evaluation of the Welding Performance

A total of 60 welded samples and 10 glued specimens were tested using a universal testing machine (MTS QT 10 KN, CMT–6104, Sans technology Inc., Shenzhen, China). The tests were carried out according to the ASTM-D 1037 standard, and the dowels were pulled out of the substrate at a rate of 2 mm/min. During a test sequence, the dowel excess was retained by a fixed chuck, while a load was applied perpendicular to the surface of the wood substrate. When the substrate block was completely pulled out, the test was stopped. Ten measurements were performed for each group, and the average values were taken as the tensile strength.

The tensile strength ($\sigma_k$ in MPa) was calculated as per the following equation [3,5]:

$$\sigma_k = \frac{F_{\max}}{S} = \frac{F_{\max}}{2\pi rh} \tag{1}$$

In Eq. (1), $F_{\max}$ is the maximum observed load (N), $S$ is the bonding surface of the sample ($mm^2$), $r$ is the radius of the pre-drilled hole (mm), and $h$ is the height of the pre-drilled hole (mm).

### 2.4 Welding Interface Temperature Measurement

During the bamboo dowel welding process, the temperature was measured using fast response thermocouples placed in the three thin holes with a diameter of 2 mm, which were predrilled through the receiving hole inner wall at a depth of 5, 10, and 15 mm from the upper surface of the poplar block (Fig. 2). A data acquisition station (model TP-K01, Yanli Automation Technology Inc., Shanghai, China) with a frequency of 100 Hz was used to measure the rise in the temperature of the welding system.

### 2.5 Scanning Electron Microscopy (SEM)

Scanning electron microscopy (SEM) micrographs of the welding interface of the bamboo dowels after testing was conducted after metallization with gold-palladium. The SEM equipment used was a Hitachi S-4800 scanning electron microscope (Tokyo, Japan).

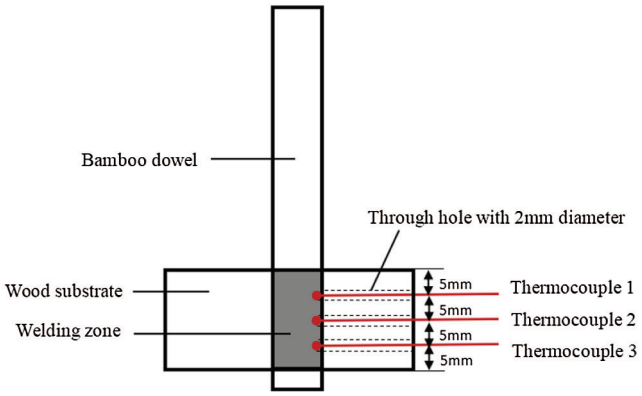


**Figure 2:** Schematic representation of the thermocouples in the heat-affected zone

### *2.6 Fourier Transform-Infrared Spectroscopy (FT-IR)*

When the dowel was inserted into the hole of the substrate block at a high speed, a large amount of molten materials will be produced because of the interference fit. Part of the high temperature molten materials remained in the gap between the dowel and hole to form a bonding line, whereas the other was expulsed from the welded interface. The expelled molten material was analyzed by FT-IR in the form of potassium bromide (KBr) pellets for their IR absorption.

The samples were ground by a ball mill, and approximately 1 mg was commingled with 300 mg of KBr to form a pellet. Before measuring the FT-IR spectra, the samples were oven dried at 100°C. The samples had particle sizes of <0.05 mm. FT-IR analyses were carried out for the raw bamboo, poplar, and expelled welding (molten) material samples by means of FT-IR spectrometer (VERTEX 80) across a wave range of 400–4000 $cm^{-1}$, wherein 16 scans were taken per spectrum with a resolution of 4 $cm^{-1}$.

## 3 Results and Discussion

### *3.1 Welding Performance*

This investigation validated the importance of the dowel/hole diameter ratio on the strength of rotation welding joints. According to Fig. 3, the tensile strength of the bamboo dowel welding joints increased with the dowel/hole diameter ratio. However, the welding strength decreased when the ratio exceeded 10/7 (1.43). In addition, an optimal ratio of 10/7 corresponding to a tensile strength as high as 7.50 MPa was observed, which differed from previous studies performed on European and North American wood dowel rotation welding that the optimal ratio was near 10/8 [1–6]. Due to the low density and high elasticity of the poplar substrate, the hole of poplar was easy to expand and deform when it was squeezed by the bamboo dowel. Therefore, a dowel/hole ratio of 10/8 was insufficient to generate enough friction. A larger ratio of 10/7 was required to ensure better contact so as to obtain a higher friction force between the dowel and hole wall. However, the ratio of 10/6 yielded excessive wear on the dowel and developed a truncated cone shape due to an excessive friction force, so as to reduce the effective bonding area of joint; thus, the tensile strength was decreased.

According to Fig. 4, the tensile strength of the bamboo dowel welded joints was higher than that of the beech dowel welded joints (6.55 MPa), schima dowel-welded joints (6.15 MPa), and PVAc glued joints (4.08 MPa). These discrepancies were due to their different anatomical structures and chemical components, which influenced the mechanical properties of the welded joints. Notably, the lignin content of the moso bamboo dowel was slightly higher than that of the other two wood dowels (Tab. 1) because most of the joint materials on the welding interface came from the dowel and not the substrate. As such, the quality of the welded joints significantly dependent on the chemical compositions and polymer

contents (particularly lignin) of the dowel [1–5]. Therefore, the abundant content of lignin in the moso bamboo was beneficial in improving the bonding performance. In addition, Shu et al. [26] reported that moso bamboo has a good physical and chemical compatibility with the poplar under high temperature conditions.

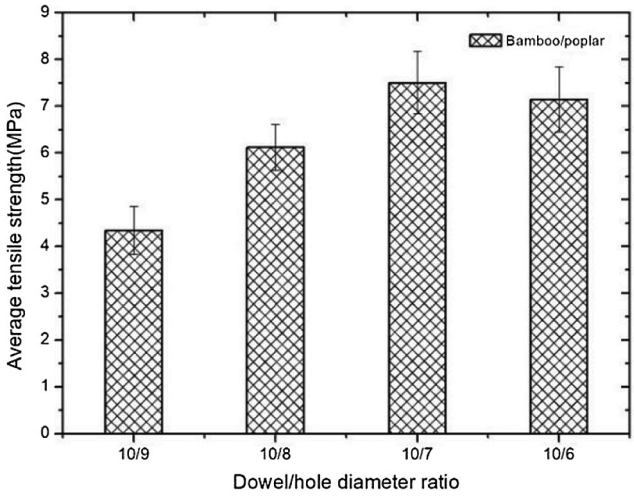


**Figure 3:** Tensile strengths of bamboo dowel welded joints with the different dowel/hole diameter ratios ($p$-value < 0.0001)

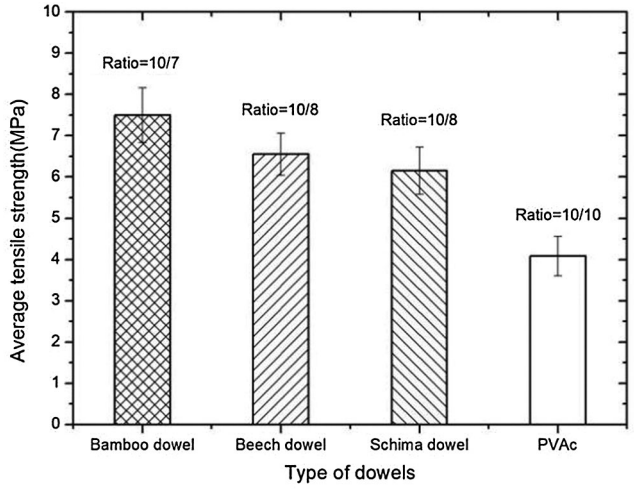


**Figure 4:** Tensile strengths of three types of dowel welded joints and PVAc glued joints with poplar substrate ($p$-value < 0.0001)

### *3.2 Temperature Measurement at the Welding Interface*

Previous studies have reported that the peak temperature in the welding interface and the welding time significantly influence the bond line quality in wood welding [2,3,5,7]. Fig. 5 illustrates the temperature change curves of the best welded joints obtained for the four dowel/hole diameter ratios, which was plotted as a function of the welding time in the welding zone. In general, the development process of the temperature curve of each ratio was roughly the same, and the temperature rose rapidly and stabilized

to the maximum in a very short period and subsequently decreased slowly due to hindered rotation (Figs. 5a–5d). The dowel and hole wall exhibited different close contacts and friction forces at the different hole depths due to differences in their dowel/hole ratios. As a result, each group exhibited three main differences: (1) Friction time (dotted line in Fig. 5), (2) Peak temperature at three monitoring hole depths, and (3) Stabilization time at the maximum temperature.

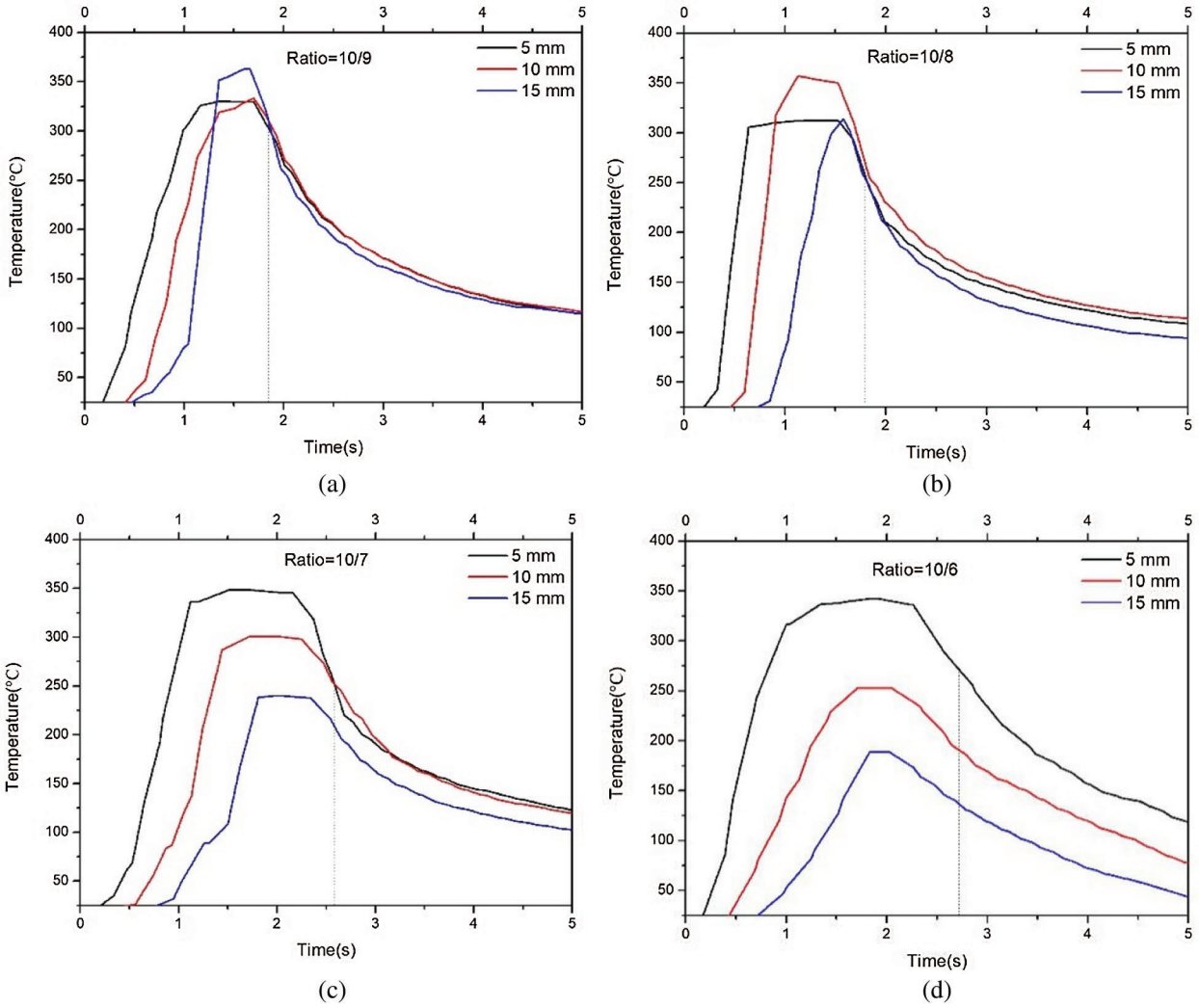


**Figure 5:** Temperature profile during bamboo dowel rotation welding, wherein the dotted line indicates the time when the rotation stopped; (a), (b), (c), and (d) are the temperature change curves increasing as a function of time at hole depths of 5, 10, and 15 mm for the cases of dowel/hole diameter ratios of 10/9, 10/8, 10/7, and 10/6, respectively

According to Figs. 5a, 5b, both the 10/9 and 10/8 diameter ratio presented a small initial friction resistance between the dowel and hole wall due to the small diameter difference and the low density substrate. In addition, the bamboo dowel exhibited a fast insertion speed and a very short friction time of less than 2 s (dotted line in Figs. 5a, 5b). The peak temperatures in three depths were between 300°C and 360°C. The stabilization period at the 5 mm, 10 mm, and 15 mm depth points were approximately 1 s, 0.5–0.8 s, and no more than 0.5 s, respectively. It was found that shorter friction times generated worse

welding effects. Two unfavorable factors deterred the ideal welding effect. First, the shorter friction time hinders the sufficient physical and chemical reaction at the welding zone. Second, the molten materials produced by friction are insufficient, thereby rendering the formation of a thick welding bond-line unfavorable, especially at the 10/9 ratio.

According to Fig. 5c, the 10/7 ratio presented friction time of more than 2.5 s (dotted line in Fig. 5c). In addition, the depths of 5 mm, 10 mm, and 15 mm exhibited peak temperatures of 348°C, 300°C, and 240°C, respectively, indicating an obvious decline in stages that corresponds to more than 1 s, 0.8 s, and 0.5 s of stabilization time, respectively. In comparison, the ratio of 10/6 presented friction time that was extended to almost 3 s (dotted line in Fig. 5d), such that the peak temperatures at 5 mm depth were 342°C, and the stabilization time at this depth was nearly extended to more than 1.5 s. Previous studies have found that the longer the welding time at the peak temperature reached, the greater the chance of burning the wood at the interface and yielding a lower strength joint [3,14], which can be explained by three reasons. First, the breakage and partial reformation of a bond may occur due to unduly prolonged welding time [1,3,7]. Second, overly extended duration at the maximum temperature increases the possibility of serious carbonization at the welding interface. Third, due to the end shape of dowel developing an obvious truncated cone appearance after an excessive period of friction, the bonding interface area of the welding dowel was seriously reduced. Furthermore, it is worth noting that, at the 15 mm monitoring point depth in Fig. 5d, the peak temperatures declined to 188°C, and the stabilization time shortened to no more than 0.5 s. Both the welding temperature and friction time significantly decreased at the bottom of hole, indicating that the close contact between the dowel and hole wall was too small to achieve the thermal softening, melting, and decomposition of the polymer materials in bamboo or wood.

The following can be seen from this investigation. (1) The friction time should be controlled between 2 and 3 s (20-mm hole depth). If the time is too long, it leads to excessive wear of the dowel and serious carbonization of the interface. If it is too short, the physical and chemical reaction at the welding zone and molten materials would be insufficient. (2) At the upper and middle parts of the pre-drilled hole (depths of 5 and 10 mm in this experiment), the peak temperatures exceeded 250–350°C, and at the bottom of the hole (a depth of 15 mm in this experiment), the welding temperature should not be lower than 150°C, so that the welding interface could reach the glass-transition temperature of lignin. (3) The optimal stabilization times of the peak temperature corresponding to the three depths were no more than 1.5 s, 1.0 s, and not less than 0.5 s, which ensured sufficient times of softening, melting, and flowing of polymer material at the welding interface in each depth.

### *3.3 Observation of the Bamboo Dowel Welding Interface*

Fig. 6a shows the poplar substrate block and the end shapes of welded bamboo dowels at the different ratios after testing. After welding, the light color of the bamboo surface welding zone at the dowel/hole diameter ratio of 10/9 was different from other dowels, and the end shape of the bamboo dowel was still almost cylindrical, indicating that both the friction and the burning were insufficient. However, the 10/6 ratio dowel developed an obvious truncated cone appearance, suggesting that the dowel achieved a sufficient friction at the initial welding stage led to a sharping shape dowel, yet the final welding stage could not obtain a high friction force due to the sharp decrease of the dowel diameter. Fig. 6b shows the surface conditions of the bamboo dowel 10/7 ratio and poplar hole wall after the tensile test. Notably, after the bamboo dowel was pulled out from the hole, some welded bamboo fibers were separated from the bamboo dowel surface, revealing the raw bamboo color and forming many grooves due to the bamboo fibers tearing. In addition, some poplar raw fibers were torn from the hole wall and bonded on the welding zone of the bamboo dowel.

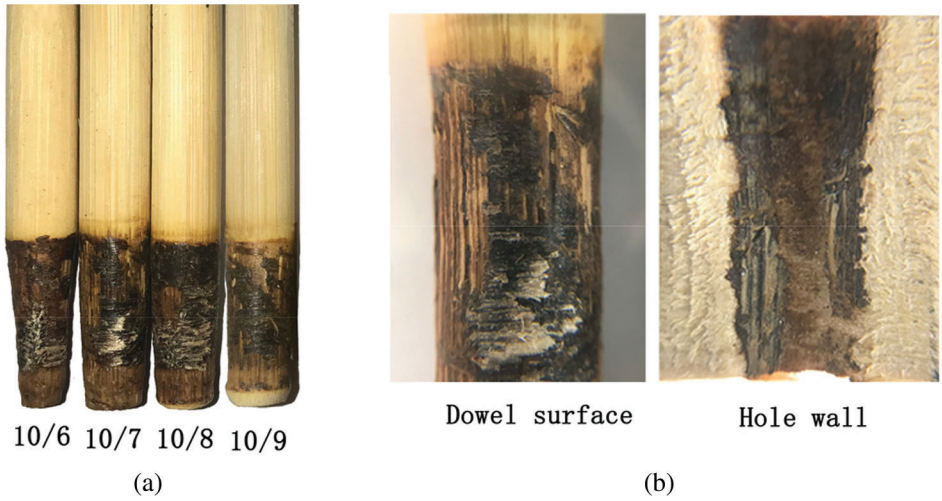


**Figure 6:** Images of tested welded specimens; (a) four bamboo dowels at dowel/hole diameter ratios of 10/6, 10/7, 10/8, and 10/9 after welding; (b) the interesting surface appearance of the bamboo dowel and poplar hole wall after testing

According to Fig. 7a, it can be easily and visibly observed that, after welding, the surfaces of the bamboo dowels were covered with a firmly layer of molten bonding interface due to the continuous rotation, friction, and compression. And it also illustrates the lifted and horizontally wound welded bamboo fibers mixed molten intercellular materials, and the right corner indicates that the longitudinal raw bamboo cells were under the welding molten layer as indicated by the arrow. The object indicated by the arrow in Figs. 7b, 7c show that the bamboo fibers, mainly the vascular bundles, were welded under the high temperature and were coated by molten materials. Fig. 7d suggests that the heat generated by the friction resulted in cell-interconnected polymer material softening, melting and flowing, thereby allowing the bamboo fibers to wrap and form a continuous and dense interface.

### *3.4 Fourier Transform-Infrared Spectroscopy (FT-IR) Analyses*

Fig. 8 presents the FT-IR spectra of the bamboo, poplar and molten materials at an optimal dowel/hole ratio of 10/7. The characteristic peaks of the molten materials were basically similar to those of the raw bamboo except for a few wavenumber absorption areas, indicating that most of the joint materials on the welding interface were derived from the bamboo dowel and not the substrate block, which was consistent with that observed in the high-speed wood dowel rotation welding [1–5]. Therefore, we focused on the changes of IR spectra of the bamboo and molten materials. As shown in Fig. 8(a), the peak produced at 3428 $cm^{-1}$ represented the hydroxyl (–OH) stretching vibration absorption peaks [16,25]. The characteristic peaks at 2920 $cm^{-1}$ and 2860 $cm^{-1}$ define the C–H stretching vibration absorption of methylene ($CH_2$) [25]. The characteristic peaks at 1000 $cm^{-1}$ to 1600 $cm^{-1}$ of the CO and $CH_2$ groups of cellulose and lignin showed slight differences between the raw bamboo and molten materials [8,16,25,30–32]. Fig. 8(b) shows the IR spectrum after baseline correction (normalized at 1055 $cm^{-1}$), which can eliminate the influence of the sample sizes on the detection. The baseline corrected spectra were then compared to the relative intensity changes of the different absorption peaks for the semi-quantitative analysis of the components. The characteristic absorption peaks at 1055 $cm^{-1}$, 1114 $cm^{-1}$ and 1424 $cm^{-1}$ represented cellulose, respectively define the C–O–C stretching vibration, C–O–C stretching vibration, and C–O bending vibration. The absorption peaks at 1514 $cm^{-1}$, 1462 $cm^{-1}$, and 1242 $cm^{-1}$ are the characteristic absorption peaks of lignin, corresponding to C=C stretching vibration, C–H bending

vibration, and C–O stretching vibration, respectively. A comparison of the relative intensities of the absorption peaks of the molten materials and moso bamboo (Fig. 8b) indicated that the IR spectra of the bamboo and molten materials were basically unchanged at 1114 $cm^{-1}$ and 1424 $cm^{-1}$ when the absorption peak of 1055 $cm^{-1}$ cellulose was used for normalization. Normalization with the 1055 $cm^{-1}$ absorption peak of cellulose ensured consistent changes in the relative content of cellulose, indicating the feasibility of selecting this peak for normalization. On the contrary, the absorption peaks at 1514 $cm^{-1}$, 1462 $cm^{-1}$, and 1242 $cm^{-1}$ were obviously enhanced, indicating that the relative content of lignin in the welding area was higher than that of raw bamboo. The wave numbers of the lignin aromatic rings increased possibly due to the condensation reactions of lignin during the heating process [8,31,33]. The thermal degradation reaction of cellulose after high temperature thermal treatment may have also induced these increases, wherein the decrease in relative cellulose content resulted in an increase in the relative lignin content. Besides, the peak splitting of cellulose at 1055 $cm^{-1}$ in the molten materials also indicated that cellulose was involved in the thermal degradation reaction. Future studies will investigate the chemical reaction mechanism of the moso bamboo dowel rotation welding technique.

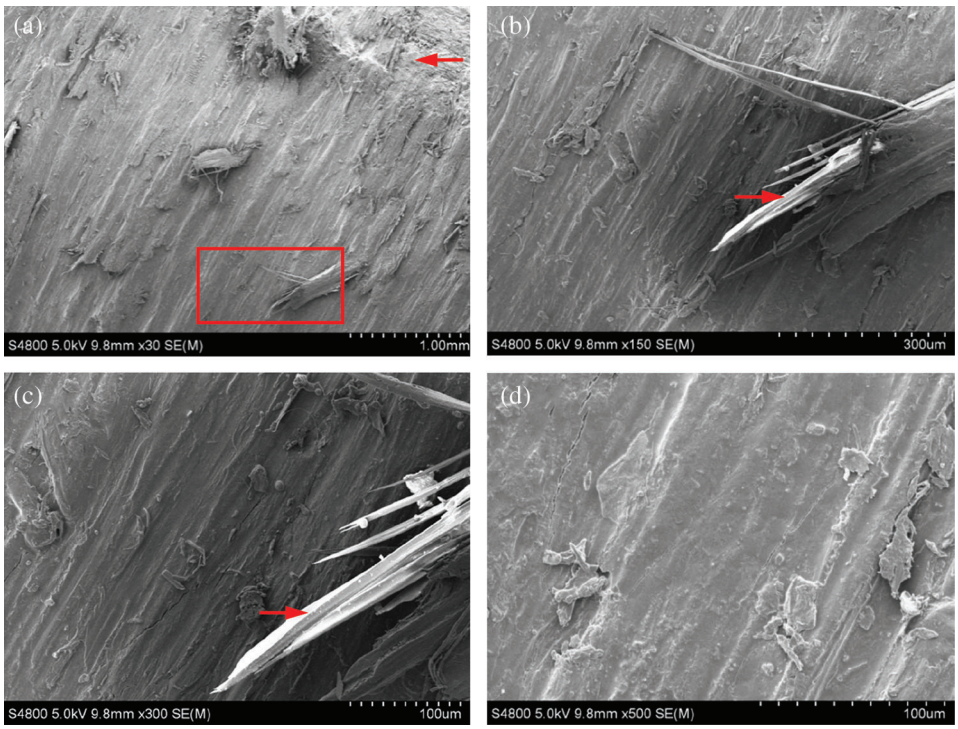


**Figure 7:** SEM micrographs of the surface of a tested bamboo-welded dowel; (a) 30x magnification showing the surface of a welded bamboo dowel; (b) detail of the same at 150x magnification showing the bamboo fibers (mainly the vascular bundles) welded under high temperature and coated by molten materials; (c) details at the same at 300x magnification; (d) details at the same 500x magnification showing a continuous and dense welding interface

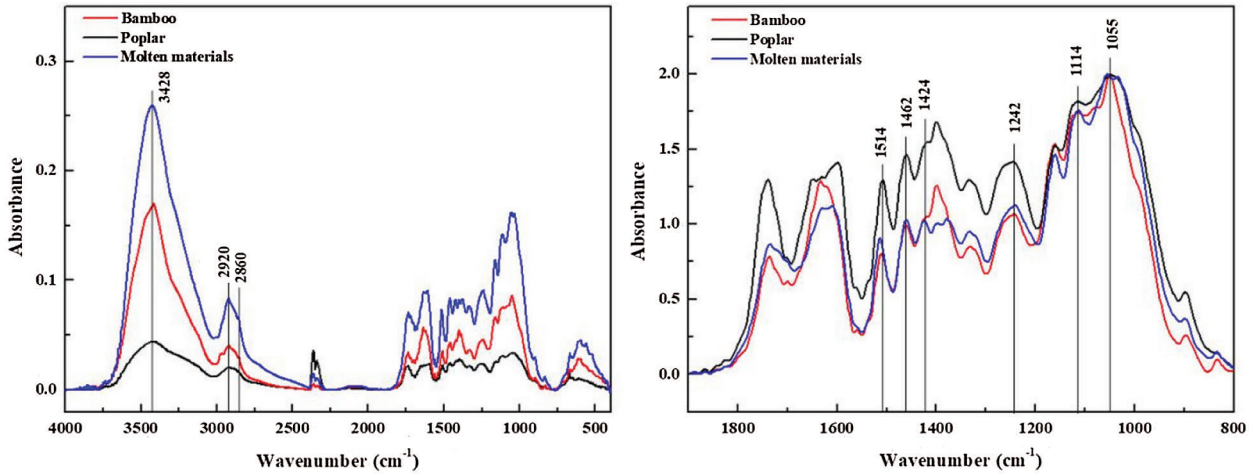


**Figure 8:** FT-IR spectra of the bamboo, poplar, and molten materials at an optimal dowel/hole ratio of 10/7; (a) non-normalized spectra from 4000 to 400 $cm^{-1}$; (b) normalized spectra from 2000 to 800 $cm^{-1}$

## 4 Conclusion

To investigate the bonding strength of a bamboo dowel to poplar substrate welded joints, a large quantity of experiments have been carried out. Due to the differences in their anatomical structures and chemical components (with abundant vascular bundles and lignin content), the tensile strength of bamboo was higher than that of beech dowel welded joints, schima dowel welded joints, and PVAc glued joints. Temperature measurement shows that the joints with a dowel/receiving hole diameter ratio of 10/7 achieve the best welding strength, i.e., the welding strength is 7.5 MPa and the peak temperatures at hole depths of 15, 10, and 5 mm reach 350°C, 300°C, and 240°C, respectively. Through microscopic analysis of the welding surface, it is found that the bonding interface is mainly composed of the intercellular components of bamboo or poplar that melt and flow under the heat generated by friction, forming components similar to reinforced concrete. The high-temperature, which was caused by high-speed rotation welding, resulted in the condensation reactions of lignin and the thermal degradation reactions of cellulose. Specifically, the relative content of lignin increased, thus improving the bonding performance. However, further experiments and methods, such as nuclear magnetic resonance and X-ray diffraction, must be performed to analyze the reaction mechanism of bamboo rotation welding.

**Acknowledgement:** Thanks to "Advanced analysis and testing center of Nanjing Forestry University" for the professional and thoughtful testing services. Any research results expressed in this paper are those of the writer(s) and do not necessarily reflect the views of the foundations.

**Funding Statement:** We thank the National Natural Science Foundation of China (31870543), the Youth Science and Technology Innovation Fund of Nanjing Forestry University (cx2016017), the National Key R&D Program of China (2017YFC0703501), the National Natural Science Foundation of China (51878590), Jiangsu Province High-level Talent Selection Training (JNHB-127), Jiangsu Provincial Department of Housing and construction (2018ZD117 and 2019ZD092), and the Natural Science Foundation of Jiangsu Province (Grant Nos. BK20170926 and BK20150878) for their funding.

**Conflicts of Interest:** The authors declare that they have no conflicts of interest to report regarding the present study.

## References


1. Pizzi, A., Leman, J. M., Kanazawa, F., Properzi, M., Pichelin, F. (2004). Wood dowel bonding by high- speed rotation welding. *Journal of Adhesion Science and Technology, 18(11),* 1263–1278. DOI 10.1163/1568561041588192.
2. Kanazawa, F., Pizzi, A., Properzi, M., Delmotte, L., Pichelin, F. (2005). Parameters influencing wood-dowel welding by high-speed rotation. *Journal of Adhesion Science and Technology, 19(12),* 1025–1038. DOI 10.1163/156856105774382444.
3. Rodriguez, G., Diouf, P., Blanchet, P., Stevanovic, T. (2011). Wood Adhesives. *Journal of Adhesion Science and Technology, 24(8/10),* 1423–1436. DOI 10.1201/b12180.
4. Ganne-Chedeville, C., Pizzi, A., Thomas, A., Leban, J. M. Bocquet, J. F. et al. (2005). Parameter interactions in two-block welding and the wood nail concept in wood dowel welding. *Journal of Adhesion Science and Technology, 19(13–14),* 1157–1174. DOI 10.1163/156856105774429037.
5. Belleville, B., Stevanovic, T., Pizzi, A., Cloutier, A., Blanchet, P. (2013). Determination of optimal wood-dowel welding parameters for two North American hardwood species. *Journal of Adhesion Science and Technology, 27 (5–6),* 566–576. DOI 10.1080/01694243.2012.687596.
6. Ivica, Z., Zoran, V., Danijela, D. (2014). Influence of various wood species and cross-sections on strength of a dowel welding joint. *Drvna Industrija, 65,* 121–127.
7. Gfeller, B., Zanetti, M., Properzi, M., Pizzi, A., Pichelin, F. et al. (2003). Wood bonding by vibrational welding. *Journal of Adhesion Science and Technology, 17(11),* 1573–1589. DOI 10.1163/156856103769207419.
8. Stamm B., Windeisen E., Natterer J., Wegener G. (2006). Chemical investigations on the thermal behaviour of wood during friction welding. *Wood Science and Technology, 40(7),* 615–627. DOI 10.1007/s00226-006-0097-2.
9. Delmott, L., Ganne-Chedeville, C., Leban, J. M., Pizzi, A., Pichelin, F. (2008). CPMAS13C NMR and FT-IR investigation of the degradation reactions of polymer constituents in wood welding. *Polymer Degradation and Stability, 93(2),* 406–412.
10. Luo, X. Y., Zhu, X. D., Zhang, J. R., Gao, Y. (2017). Theoretical research and technical progress of wood welding. *Journal of Northwest Forestry University, 32(6),* 270–275 (in Chinese).
11. Renaud, A. (2009). Minimalist Z chair assembly by rotational dowel welding. *European Journal of Wood and Wood Products, 67(1),* 111–112. DOI 10.1007/s00107-008-0264-2.
12. Bocquet, J. F., Pizz, A., Despres, A., Mansouri, H. R., Tesch, L. et al. (2007). Wood joints and laminated wood beams assembled by mechanically-welded wood dowels. *Journal of Adhesion Science and Technology, 21(3-4),* 301–317. DOI 10.1163/156856107780684585.
13. Bocquet, J. F., Pizzi, A., Resch, L. (2007). Full-scale industrial wood floor assembly and structures by welded-through dowels. *Holz als Roh-und Werkstoff, 65(2),* 149–155. DOI 10.1007/s00107-006-0170-4.
14. Resch, L., Despres, A., Pizzi, A., Bocquet, J. F., Leban, J. M. (2006). Welding-through doweling of wood panels. *Holz als Roh- und Werkstoff, 64(5),* 423–425.
15. O'Loinsigh, C., Oudjene, M., Ait-Aider, H., Fanning, P. (2012). Experimental study of timber-to-timber composite beam using welded-through wood dowels. *Construction and Building Materials, 36,* 245–250. DOI 10.1016/j.conbuildmat.2012.04.118.
16. Shu, B., Ren, Q., He, Q., Ju, Z. Zhan, T. et al. (2019). Study on mixed biomass binderless composite based on simulated wood. *Wood Research, 64(6),* 1023–1034.
17. Zhang, S. J. (2017). *Application of fast-growth wood in light wood frame construction (Ph.D. Thesis)*. Nanjing Forestry University.
18. Zhang, Q. S. (1995). *Industrial utilization of bamboo in China*. Beijing: China Forestry Publishing House.
19. Jiang, Z. H. (2002). *World bamboo and rattan*. Liaoning: Liaoning Science & Technology Press.
20. Wu, X. Z., Huang, X. Y., Li, X. J., Wu, Y. Q. (2019). Flexural performance of CFRP-bamboo scrimber composite beams. *Journal of Renewable Materials, 7(12),* 1295–1307. DOI 10.32604/jrm.2019.07839.
21. Fang, C. H., Jiang, Z. H., Sun, Z. J., Liu, H. R., Zhang, X. B. et al. (2018). An overview on bamboo culm flattening. *Construction and Building Materials, 171,* 65–74. DOI 10.1016/j.conbuildmat.2018.03.085.

22. Li, H. T., Qiu, Z. Y., Wu, G., Corbi, O., Wang, L. B. et al. (2019). Slenderness ratio effect on eccentric compression performance of parallel strand bamboo lumber columns. *Journal of Structural Engineering, 145(8),* 04019077.
23. Hu, J. B., Pizzi, A. (2013). Wood-bamboo-wood laminated composite lumber jointed by linear vibration-friction welding. *European Journal of Wood, 71(5),* products,71,683–products,71,686. DOI 10.1007/s00107-013-0714-3.
24. Zhang, H. Y., Pizzi, A., Lu, X. N., Zhou, X. H. (2014). Optimization of tensile shear strength of linear mechanically welded outer-to-inner flattened moso bamboo (Phyllostachys pubescens). *BioResources, 9(2),* 2500–2508.
25. Zhang, H. Y. (2014). *The study of linear vibration welding of moso bamboo (Ph.D. Thesis)*. Nanjing Forestry University, Nanjing.
26. Zhang, H., He, Q., Lu, X., Pizzi, A. Mei, C. et al. (2017). Energy release rate measurement of welded bamboo joints. *Journal of Renewable Materials, 8(6),* 450–456. DOI 10.7569/JRM.2017.634180.
27. Li, H., Zhang, H., Qiu, Z., Su, J. Wei, D. et al. (2020). Mechanical properties and stress strain relationship models for bamboo scrimber. *Journal of Renewable Materials, 8(1),* 13–27. DOI 10.32604/jrm.2020.09341.
28. Antonovic, A., Jambrekovic, V., Pervan, S., Istvanic, J., Greger, K. et al. (2008). A supplement to the research of native lignin of beech sapwood (*Fagus sylvatical*). *Wood Research, 53,* 1, 55–1, 68.
29. Li, L., Wang, C. M. (2008). Study on the chemical component and variation of wood Schima wallichii under plantation. *Shandong Forestry Science and Technology, 2,* 5–8 (in Chinese).
30. Zhang, J. R., Gao, Y., Xu, L., Luo, X. Y., Zhu, X. D. (2017). Properties and mechanism of larch with wood-dowel rotation welding. *Journal of Northwest Forestry University, 32(4),* 229–234 (in Chinese).
31. Faix, O. (1992). Fourier transform infrared spectroscopy. In: Lin, S. Y., Dence, C. W. (eds.), *Methods in Lignin Chemistry,* pp. 83–109. Berlin, Heidelberg, New York: Springer.
32. Xu, G., Wang, L., Liu, J., Wu, J. (2013). FTIR and XPS analysis of the changes in bamboo chemical structure decayed by white-rot and brown-rot fungi. *Applied Surface Science, 280,* 799–805. DOI 10.1016/j. apsusc.2013.05.065.
33. Elisabeth, W., Gerd, W. (2008). Behaviour of lignin during thermal treatments of wood. *Industrial Crops and Products, 27,* 157–162.